

알칼리용액에서 산소환원 및 발생반응에 대한 $\text{La}_{0.8}\text{Sr}_{0.2}\text{CoO}_3$ 전극의 기체확산층 영향

로페즈 카린¹ · 양진현¹ · 선호정² · 박경세³ · 엄승욱⁴ · 임형렬⁵ · 이홍기⁵ · 심종표^{1†}

¹군산대학교 나노화학공학과, ²군산대학교 신소재공학과, ³군산대학교 화학과,
⁴한국전기연구원 전지연구센터, ⁵우석대학교 수소연료전지 지역혁신센터

Effect of Gas Diffusion Layer on $\text{La}_{0.8}\text{Sr}_{0.2}\text{CoO}_3$ Bifunctional Electrode for Oxygen Reduction and Evolution Reactions in an Alkaline Solution

KAREEN J. LOPEZ¹, JIN-HYUN YANG¹, HO-JUNG SUN², GYUNGSE PARK³,
SEUNGWOOK EOM⁴, HYUNG-RYUL RIM⁵, HONG-KI LEE⁵, JOONGPYO SHIM^{1†}

¹Department of Nano & Chemical Engineering

²Material Science & Engineering

³Chemistry, Kunsan National University, Jeonbuk, 54150, Korea

⁴Battery Research Center Korea Electrotechnology Research Institute, Changwon, Gyeongnam, 51543, Korea

⁵Fuel Cell Regional Innovation Center, Woosuk University, Jeonbuk, 55315, Korea

Abstract >> Various commercially available gas diffusion layers (GDLs) from different manufacturers were used to prepare an air electrode using $\text{La}_{0.8}\text{Sr}_{0.2}\text{CoO}_3$ perovskite (LSCP) as the catalyst for the oxygen reduction reaction (ORR) and oxygen evolution reaction (OER) in an alkaline solution. Various GDLs have different physical properties, such as porosity, conductivity, hydrophobicity, etc. The ORR and OER of the resulting cathode were electrochemically evaluated in an alkaline solution. The electrochemical properties of the resulting cathodes were slightly different when compared to the physical properties of GDLs. Pore structure and conductivity of GDLs had a prominent effect and their hydrophobicities had a minor effect on the electrochemical performances of cathodes for ORR and OER.

Key words : Perovskite(페로브스카이트), $\text{La}_{0.8}\text{Sr}_{0.2}\text{CoO}_3$, catalyst(촉매), gas diffusion layer(기체확산층), oxygen reduction(산소환원), oxygen evolution(산소발생)

1. Introduction

The oxygen reduction reaction (ORR) and oxygen evolution reaction (OER) in an alkaline solution have

been extensively studied in the past due to its significance in several renewable energy conversion and storage devices. Metal-air batteries, like zinc-air battery, are among the energy storage devices that have attracted much attention because of their high specific energy, low cost, and safe operation. At present, primary zinc-air battery is commercially available,

[†] Corresponding author : jpschim@kunsan.ac.kr

Received : 2016.10.19 in revised form : 2016.12.3 Accepted : 2016.12.30

Copyright © 2016 KHNES

whereas the rechargeable one is still under study because of several critical problems. The poor performance of ORR and OER in the air electrode is one of the major drawbacks¹⁻⁷. Catalyst layer and GDL comprises the bifunctional air electrode wherein the catalyst for ORR and OER is located at catalyst layer and the GDL allows the diffusion of atmospheric oxygen necessary for the reaction to take place. In an effort to address the limitation of the current zinc-air battery, several researches were made to find a catalyst that can effectively catalyze both the ORR and OER; such catalysts are termed bifunctional catalyst. Pt and Pt-Ru catalysts have shown the highest catalytic activity for ORR and OER but, because of their high cost and other drawbacks, non-noble metal catalysts such as perovskites are preferred, among which $\text{La}_{1-x}\text{Sr}_x\text{CoO}_3$ exhibits the highest catalytic activity⁸⁻¹¹.

The performance of an air electrode is not only affected by a bifunctional catalyst but also requires effective diffusion of O_2 through GDL and interaction between catalyst and supporting layer¹¹. A GDL should have the ability to transport oxygen from the atmosphere to the catalyst layer and possess low electronic resistance, good electrical conductivity, and excellent wetting characteristics^{12,13}. The GDL of a zinc-air battery is usually composed of a pressed mixture of carbon powder as the support material, a binder for providing mechanical stability, and/or a hydrophobic additive to avoid electrolyte leakage¹⁴. However, the GDL often used in polymer electrolyte membrane fuel cells (PEMFCs) and alkaline fuel cells (AFCs) can also be used in zinc-air batteries. In PEMFCs, GDLs are commonly fabricated with carbon materials because of its low density and high surface area¹⁵. The carbon material can be in the form of a cloth or paper, with

or without polytetrafluoroethylene (PTFE) treatment as a wet-proofing agent, and microporous layer (MPL), which can improve the efficiency of the catalyst and minimize the possible electrode flooding¹⁶⁻¹⁸. Usually, the cell performance of bifunctional electrode for ORR and OER in alkaline solution has been focused on the catalytic activities of materials. There has been little work for the effect of GDL in electrochemical systems using alkaline solution, even though gas diffusion would be very important in bifunctional electrode and there are many literatures about the role of GDL in PEMFCs.

In this study, various commercial GDLs were investigated for their potential influence on the electrochemical performance of an air electrode that employs $\text{La}_{0.8}\text{Sr}_{0.2}\text{CoO}_3$ perovskite (LSCP) as the bifunctional catalyst for ORR and OER in an alkaline solution. Furthermore, the relationships between electrochemical performances and physical properties of GDLs have also been summarized.

2. Experimental

Catalyst layer consisted of LSCP powder (LSC-P, Fuel Cell Materials), PTFE (60% dispersion, DuPont), carbon black (CB) (Vulcan XC-72R, Cabot), Ni powder (255, Vale). GDLs were obtained from three companies. The preparation of electrode involves two steps: the preparation of catalyst layer and combining of catalyst layer and GDL. It was prepared by mixing the LSCP catalyst with Ni powder and CB. Then distilled water and ethanol were added and the resulting mixture was ultrasonicated for 5 min with occasional stirring to ensure proper dispersion followed by the addition of PTFE suspension and the slurry was mechanically

Table 1 Physical properties of different GDLs supplied from manufacturers

Manufacture Name	Sample	Type	Thickness (μm)	Density (g/cm^3)	PTFE treated	Porosity (%)	Permeability ($\text{cm}^3/(\text{cm}^2 \cdot \text{s} \cdot \text{air})$)	Resistance ($\text{m}\Omega \cdot \text{cm}^2$)	MPL
Ballard GDS1120	BP11	paper	184	0.4	8~15%		210sec/100cc	<14.5	O
Ballard GDS2120	BP21	paper	260	0.4	8~15%		145sec/100cc	<14.0	O
SGL 10BC	SP10	paper	420	0.32	5%	82	1.45	<16 at 1 MPa	O
SGL 25BC	SP25	paper	235	0.37	5%	80	1.0	<12 at 1 MPa	O
Ballard P50	BP50	paper	180	0.34	15%		50sec/100cc	11.7	X
Toray TGP-H-060	TP60	paper	190	0.44	yes	78		80($\text{m}\Omega \cdot \text{cm}$)	X

stirred for another 10 min. It was then oven dried at 60°C. Once the solvent was removed, a paste was made using isopropyl alcohol (IPA, Aldrich), which was then rolled into a sheet and dried for an hour to remove IPA. The dried catalyst layer was hot-pressed with GDL for 5min at 350°C and 1MPa.

The physical properties of the different GDLs are shown in Table 1. The information was obtained from their respective manufacturers^{17,19}. In addition, the morphologies of various GDLs were determined using field emission-scanning electron microscopy (FE-SEM, S-4800, Hitachi) and their contact angles were measured using ImageJ software with a Drop analysis plugin: Drop Snake on an obtained image containing a drop of water on the GDL²⁰. The in-plane sheet resistances of GDLs were measured using the four-point probe method with a conductivity meter (Changmin Tech, CMT-SR-100N). The air flux through a plane (along the z direction) of the GDLs was measured with a lab-made permeometer using ASTM D737: the air flow per minute was measured at a water pressure drop of 1.27 cm (0.5 inch) between the gas inlet and outlet. The air permeability was calculated according to Darcy' law²¹⁻²³.

The electrochemical characterizations of bifunctional electrodes for ORR and OER were derived from our previous studies^{24,25}. The apparent active area of electrode in contact with the electrolyte was 1.0 cm^2 . It was assembled into a three-electrode cell including the working electrode with Zn wire and Pt mesh as the reference and the counter electrode. The electrolyte used was 8 M KOH solution. The analysis of ORR and OER performance was conducted by linear sweep voltammetry (LSV) for 20 cycles using potentiostat/galvanostat (WBCS 3000, WonATech) with a potential ranging from 0.5 to 2.4V (vs. Zn/Zn^{2+}) and a scan rate of 1mV/s.

3. Results and discussion

The physical properties of various GDLs shown in Table 1 indicate the similarity of BP50 and BP11 in which their base substrate is the same Teflonated or PTFE treated carbon paper. Fig. 1a-f are the SEM images of the paper-type GDLs, in which surfaces of BP11 (Fig. 1a) and BP21 (Fig. 1b) appear as agglomerated particles. Similarly, SEM images of SP10 (Fig. 1c) and SP25 (Fig. 1d) are observed to have more compact

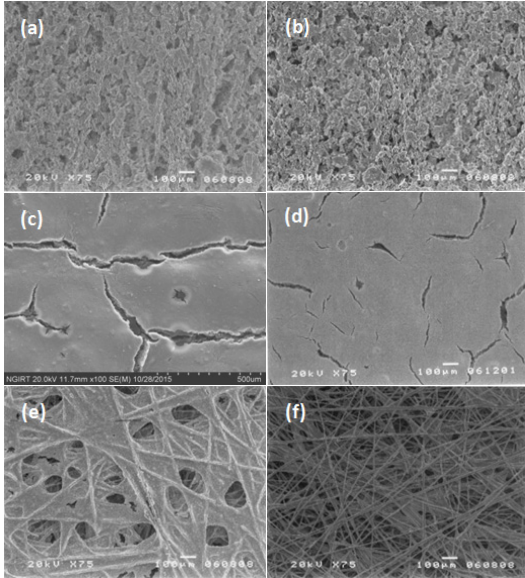


Fig. 1 SEM images of various GDLs (a) BP11, (b) BP21, (c) SP10, (d) SP25, (e) BP50 and (f) TP60

particle agglomeration, and show cracks, making them less porous. From Table 1, it can be inferred that the agglomerated particles observed in Fig. 1a-d constitute the microporous layer applied on GDLs. In SEM images of BP50 (Fig. 1e) and TP60 (Fig. 1f), they are highly porous due to randomly arranged carbon fibers. It can be noted that the fibers of TP60 are significantly smaller than BP50, and even when both are PTFE-treated, the wet-proofing treatment is more evident from the SEM image of BP50 (Fig. 1e)^{16,19}.

The surface appearance of the various GDLs in Fig. 1 also revealed the difference between BP11 (Fig. 1a) and BP50 (Fig. 1e). The BP11 has MPL on one side of BP50, while the other side is almost identical to BP50. The application of MPL to BP50 gradually increased its thickness and density while the permeability decreased four times. BP21 is similar to BP11 in that both have MPL on a PTFE-treated substrate, but the difference between the two is that BP21 has a thicker carbon paper substrate. Similarly, SP10 and SP25

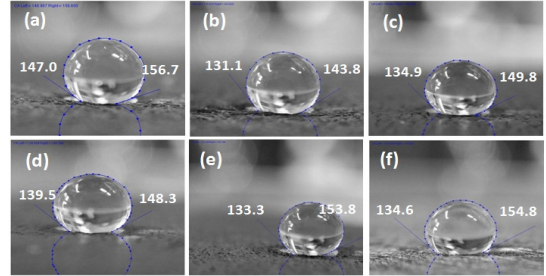


Fig. 2 Image J with Drop analysis: Drop Snake plug-ins for Contact Angle measurements of various GDLs (a) BP11, (b) BP21, (c) SP10, (d) SP25, (e) BP50 and (f) TP60

(same manufacturer) are both graphitized carbon-fiber-based non-woven paper that are 5% PTFE-treated with a standard micro porous layer on one side. Front and back surface image of SP10 and SP25 has no distinguishable difference between each other; however, as described by their manufacturer, SP25 seemed to be a more developed version of SP10. TP60 (Fig. 1f) is another PTFE-treated carbon paper without MPL^{17,19,26}.

Waterproofing or PTFE treatment of carbon substrates for GDLs has been used to avoid possible disruption of air transport that happens when water blocks the pores of GDL¹⁹. Fig. 2 shows the image of a water drop on the surface of GDLs along with the approximated contact angle determined using the software ImageJ drop analysis, drop snake. All GDLs were confirmed to have non-wetting property and the most hydrophobic GDL is BP11 (Fig. 2a)^{20,27}.

The electrochemical characteristics of LSCP catalyst with various GDLs for ORR and OER at the 20th cycle are shown in Fig. 3. The BP series showed better performance than others for ORR and OER. The performances of electrodes with SP25, SP10, and TP60 were relatively lower for both ORR and OER. Fig. 4 shows the average current as a function of GDL types at 0.5V and 2.4V for ORR and OER, respectively, which were collected over more than 4 cell tests.

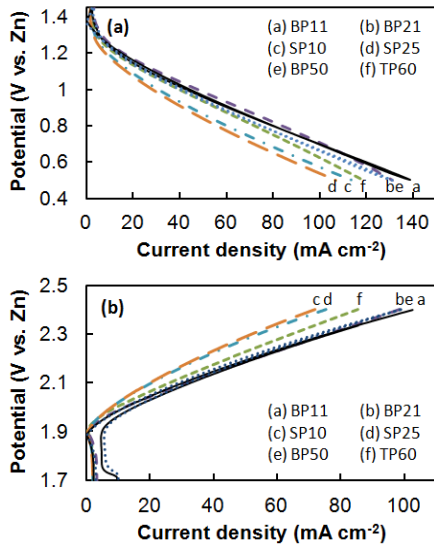


Fig. 3 Linear sweep voltammograms of bifunctional electrodes with different GDLs at the 20th cycle for (a) ORR and (b) OER

Fig. 5 and 6 show the correlation of currents at 0.5V and 2.4V for the ORR and OER as a function of physical properties of various GDLs. Both figures exhibit similar tendency. For the ORR, the current increased with increasing porosity, pore size, in-plane resistivity and PTFE content, but air permeability showed contrary behavior. Porosity decreases mass transfer polarization losses in gas diffusion electrodes²⁸. Other interesting features are the variation of current with air permeability and resistivity. The air permeabilities of GDLs, which were measured by method described in this work, were in the range of 0.18-0.64 cc/cm²·min. The air flow for 100 mA/cm² is theoretically 1.74 cc/cm²·min, which is higher than the air permeabilities of the GDLs tested. Therefore, the driving force for air into or out of the electrode is the concentration gradient caused by the consumption or production of oxygen during ORR or OER, respectively. The measured air permeabilities may not correlate to the change in current, but pore structure may directly

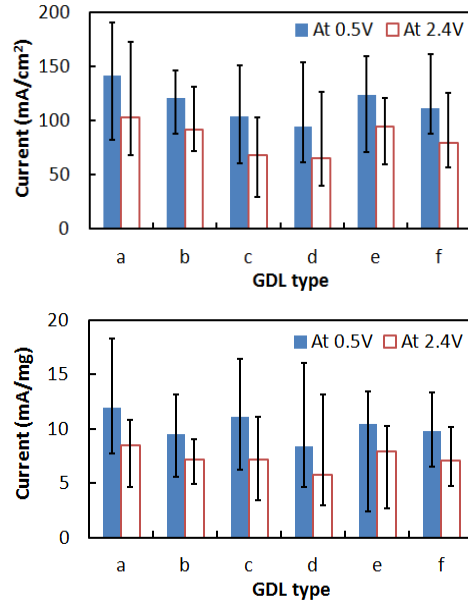


Fig. 4 Current based on electrode area (left) and catalyst mass (right) of LSCP cathodes with various GDLs at the 20th cycle. (a) BP11, (b) BP21, (c) SP10, (d) SP25, (d) BP50 and (f) TP60

affect the diffusion of oxygen or air and this could influence the OER. Furthermore, the current increased with increasing resistivities of GDLs. The difference of cell potential induced by the ohmic resistance of electrode is 20 - 65mV and these potential drops may not determine the cell performance. The hydrophobic property of the electrode is also important due to the blocking of gas diffusion pathway by electrolyte solution²⁹. As shown in Fig. 5, the current increased slightly with increasing PTFE content in GDL. However, the contact angles of different GDLs were almost same implying that they are hydrophobic enough to repel water. Labato et al. and Prasanna et al. independently reported that 10 - 20% PTFE in carbon paper improved the mechanical properties of the carbon support and caused a very small drop in the performance of the PEMFCs^{30,31}.

The electrochemical behaviors of LSCP with BP50

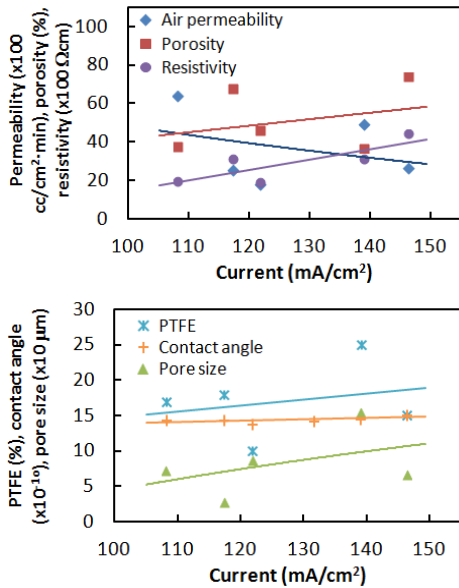


Fig. 5 Relationship between current at 0.5 V and physical properties of various GDLs

and BP11 GDLs show the positive contribution of MPL on the overall performance of an electrode. The addition of MPL on the carbon substrate improves the efficiency of the GDL. However, other physical properties like air permeability, porosity, and thickness contribute as well, as manifested by the difference in the electrode performance between BP11 and BP21. The thickness and weight of BP11 are smaller than BP21, however, its air permeability and conductivity are higher. The lower thickness and higher air permeability of BP11 may have provided a better oxygen transport from the atmosphere to the catalyst layer resulting in better performance of BP11 than BP21. This explains to the lower electrochemical performance of LSCP with SP10 and SP25 despite being PTFE treated and possessing MPL.

4. Conclusions

To conclude, the ORR and OER performance of

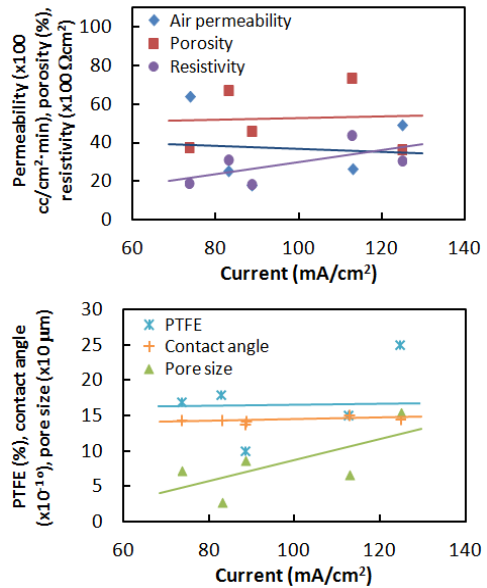


Fig. 6 Relationship between current at 2.4 V and physical properties of various GDLs

LSCP in alkaline solution varied with different types of GDLs and certain physical properties of the GDLs can have a significant influence when present in a specific type of GDL. Moreover, physical properties of GDLs, such as thickness, porosity, air permeability, conductivity, wet-proofing, and MPL coating have resulted in a higher ORR and OER performance of an air electrode. The results have shown that electrode with paper-type BP11 GDL with thinnest thickness offers the highest ORR and OER performance in alkaline solution due to air could be permeable easily through shortest path in GDL, and that cell performance may be affected by pore structure of electrode including GDL and catalyst layer.

Acknowledgement

This work was supported by the National Research Foundation of Korea Grant funded by the Korean Government (MEST) (NRF-2012-M1A2A2-029538).

References

1. M. Li, L. Zhang, Q. Xu, J. Niu, Z. Xia, "N-doped graphene as catalysts for oxygen reduction and oxygen evolution reactions: Theoretical considerations", *J. Catalysis*, Vol. 314, 2014, p.66.
2. J. Lee, B. Jeong, J.D. Ocon, "Oxygen electrocatalysis in chemical energy conversion and storage technologies", *Curr. Appl. Phys.*, Vol. 13, 2013, p. 309.
3. C.A.C. Sequeira, D.M.F. Santos, W.Baptista, "Oxygen reduction at a manganate electrocatalyst in KOH solutions", *J. Braz. Chem. Soc.*, Vol. 17, 2006, p.910.
4. X. Li, W. Qu., J. Zhang, H. Wang, "Electrocatalytic Activities of Perovskite toward Oxygen Reduction Reaction in Concentrated Alkaline Electrolytes", *ECS Transactions*, Vol. 28, 2010, p. 45.
5. H.W. Park, D.U. Lee, P. Zamani, M.H. Seo, L.F. Nazar, Z. Chen, "Electrospun porous nanorod perovskite oxide/nitrogen-doped graphene composite as a bi-functional catalyst for metal air batteries", *Nano Energy*, Vol. 10, 2014, p. 192.
6. X. An, D. Shin, J.D. Ocon, J.K. Lee, Y. Son, J. Lee, "Electrocatalytic oxygen evolution reaction at a FeNi composite on a carbon nanofiber matrix in alkaline media", *Chinese J. Catalysis*, Vol. 35, 2014, p. 891.
7. D. Zhang, Y. Song, Z. Du, L. Wang, Y. Li, J.B. Goodenough, "Active $\text{LaNi}_{1-x}\text{Fe}_x\text{O}_3$ bifunctional catalysts for air cathodes in alkaline media", *J. Mater. Chem. A*, Vol. 3, 2015, p. 9421.
8. V. Caramia, B. Bozzini, "Materials science aspects of zinc-air batteries: a review", *Mater Renew Sustain Energy*, Vol. 3, 2014, p. 28.
9. S.H. Lee, Y. Jeong, S. Lim, E. Lee, C. Yi, K. Kim, "The Stable Rechargeability of Secondary Zn-Air Batteries: Is It Possible to Recharge a Zn-Air Battery?", *J. Kor. Electrochem. Soc.*, Vol. 13, 2010, p. 45.
10. X. Wang, P.J. Sebastian, M.A. Smit, H. Yang, S.A. Gamboa, "Studies on the oxygen reduction catalyst for zinc-air battery electrode", *J. Power Sources*, Vol. 124, 2003, p. 278.
11. R.D. McKerracher, C. Alegre, V. Baglio, A.S. Arico, C. P. de Leon, F. Mornaghini, M. Rodlert, F.C. Walsh, "A nanostructured bifunctional Pd/C gas-diffusion electrode for metal-air batteries", *Electrochim. Acta*, Vol. 174, 2015, p. 508.
12. N. Parikh, J.S. Allen, R.S. Yassar, "Microstructure of Gas Diffusion Layers for PEM Fuel Cells", *Fuel Cells*, Vol. 12, 2012, p. 382.
13. E. Sengul, S. Erkan, I. Eroglu, N. Bac, "Effect of Gas Diffusion Layer Characteristics and Addition of Pore-Forming Agents on the Performance of Polymer Electrolyte Membrane Fuel Cells", *Chem. Eng. Comm.*, Vol. 196, 2008, p. 161.
14. T. Wang, M. Kaempgen, P. Nopphawan, G. Wee, S. Mhaisalkar, M. Srinivasan, "Silver nanoparticle-decorated carbon nanotubes as bifunctional gas-diffusion electrodes for zinc-air batteries", *J. Power Sources*, Vol. 195, 2010, p. 4350.
15. T. Kim, T. Xie, W. Jung, F. Gadala-Maria, P. Ganesan, B.N. Popov, "Development of catalytically active and highly stable catalyst supports for polymer electrolyte membrane fuel cells", *J. Power Sources*, Vol. 273, 2015, p. 761.
16. M.J. Martinez-Rodriguez, T. Cui, S. Shimpalee, S. Seraphin, B. Duong, J.W. Van Zee, "Effect of microporous layer on MacMullin number of carbon paper gas diffusion layer", *J. Power Sources*, Vol. 207, 2012, p. 91.
17. J. Lee, I. Kim, Y. Zhang, H. Lee, J. Shim, "Comparison of Cell Performance with Physical Properties of Gas Diffusion Layers in PEMFCs", *J. Kor. Electrochem. Soc.*, Vol. 10, 2007, p. 270.
18. C. Lim, C.Y. Wang, "Effects of hydrophobic polymer content in GDL on power performance of a PEM fuel cell", *Electrochim. Acta*, Vol. 49, 2004, p. 4149.
19. A. El-karouf, T.J. Mason, D.J.L Brett, B.G. Pollet,

- “Ex-situ characterisation of gas diffusion layers for proton exchange membrane fuel cells”, *J. Power Sources*, Vol. 218, 2012, p. 393.
20. A.F. Stalder, G. Kulik, D. Sage, L. Barbieri, P. Hoffmann, “A snake-based approach to accurate determination of both contact points and contact angles”, *Coll. Surf. A: Physicochem. Eng. Aspects*, Vol. 286, 2006, p. 92.
 21. Dullien FAL, “Porous Media: Fluid Transport and Pore Structure”, Academic Press, New York, 1992.
 22. J. Geertsma, “Estimating the coefficient of inertial resistance in fluid flow through porous media”. *Soc Pet Eng J*, Vol. 10, 1974, p. 445.
 23. J. Shim, C. Han, H.J. Sun, G. Park, “Preparation and Characterization for Carbon Composite Gas Diffusion Layer on Polymer Electrolyte Membrane Fuel Cells”. *Trans Kor Hydrogen New Energy Soc*, Vol. 23, 2012, p. 34.
 24. K. Lopez, G. Park, H.J. Sun, J.C. An, S. Eom, J. Shim, “Electrochemical characterizations of LaMO_3 ($M = \text{Co}, \text{Mn}, \text{Fe}, \text{and Ni}$) and partially substituted $\text{LaNi}_x\text{M}_{1-x}\text{O}_3$ ($x = 0.25$ or 0.5) for oxygen reduction and evolution in alkaline solution”, *J. Appl. Electrochem.*, Vol. 45, 2015, p. 313.
 25. J. Shim, K. J. Lopez, H.-J. Sun, G. Park, J.-C. An, S. Eom, S. Shimpalee, J.W. Weidner, “Preparation and characterization of electrospun LaCoO_3 fibers for oxygen reduction and evolution in rechargeable Zn-air batteries”, *J. Appl. Electrochem.*, Vol. 45, 2015, p. 1005.
 26. X.L. Wang, H.M. Zhang, J.L. Zhang, H.F. Xu, Z.Q. Tian, J. Chen, H.X. Zhong, Y.M. Liang, B.L. Yi, “Micro-porous layer with composite carbon black for PEM fuel cells”, *Electrochim. Acta*, Vol. 51, 2006, p. 4909.
 27. X.F. Wu, Y.A. Dzenis, “Droplet on a fiber: geometrical shape and contact angle”, *Acta Mechanica*, Vol. 185, 2006, p. 215.
 28. G. Selvarani, A. K. Sahu, P. Sridhar, S. Pitchumani, A. K. Shukla, “Effect of diffusion-layer porosity on the performance of polymer electrolyte fuel cells”, *J. Appl. Electrochem.*, Vol. 38, 2008, p. 357.
 29. E.L. Gyenge and J.-F. Drillet, “The Electrochemical Behavior and Catalytic Activity for Oxygen Reduction of MnO_2/C Toray Gas Diffusion Electrodes”, *J. Electrochem. Soc.*, Vol. 159, 2012, p. F23.
 30. J. Lobato, P. Canizares, M. A. Rodrigo, C. Ruiz-Lopez, J. J. Linares, “Influence of the Teflon loading in the gas diffusion layer of PBI-based PEM fuel cells”, *J. Appl. Electrochem.*, Vol. 38, 2008, p. 793.
 31. M. Prasanna, H.Y. Ha, E.A. Cho, S.-A. Hong, I.-H. Oh, “Influence of cathode gas diffusion media on the performance of the PEMFCs”, *J. Power Sources*, Vol. 131, 2004, p. 147.